Redox-Linked Protonation of Cytochrome *c* Oxidase: The Effect of Chloride Bound to Cu_B[†]

Elena Forte,[‡] Maria Cecilia Barone,[‡] Maurizio Brunori, Paolo Sarti,* and Alessandro Giuffrè

Department of Biochemical Sciences and CNR Institute of Molecular Biology and Pathology, University of Rome "La Sapienza", I-00185 Rome, Italy

Received April 3, 2002; Revised Manuscript Received June 21, 2002

ABSTRACT: The effect of bound Cl^- on the redox-linked protonation of soluble beef heart cytochrome *c* oxidase (CcOX) has been investigated at pH 7.3−7.5 by multiwavelength stopped-flow spectroscopy, using phenol red as the pH indicator in an unbuffered medium. Reduction by Ru-II hexamine of the Cl-bound enzyme is associated with an overall apparent uptake of 1.40 ± 0.21 H^+/aa_3, whereas 2.28 ± 0.36 H^+/aa_3 is taken upon reduction of the Cl-free enzyme. Bound Cl^- has no effect on the extent of H^+ uptake coupled to heme *a* reduction (0.59 ± 0.06 H^+/aa_3), but significantly decreases (by ∼0.9 H^+/aa_3) the apparent stoichiometry of H^+ uptake coupled to heme a_3-Cu_B reduction, by eliminating the net H^+ uptake linked to Cu_B reduction. To account for these results, we propose that, after the transfer of the first electron to the active site, reduction of Cu_B is associated with Cl^- dissociation, addition of a H^+, and diffusion into the bulk (with subsequent dissociation) of HCl. In the physiologically competent Cl^--free enzyme, an OH^- likely bound to oxidized Cu_B is protonated upon arrival of the first electron, and dissociates as H_2O. The relevance of this finding to the understanding of the enzyme mechanism is discussed.

Cytochrome *c* oxidase (CcOX),[1] the terminal electron acceptor of the respiratory chain, catalyzes the exoergonic electron transfer from cytochrome *c* to O_2 to form H_2O. The reaction is coupled to an active translocation of protons and generates a proton motive force used for ATP synthesis (see refs *1*−*3* for reviews). Oxygen chemistry takes place at the binuclear active site (heme a_3-Cu_B), the reduction of which occurs via intramolecular electron transfer from heme *a*; this is in turn reduced by Cu_A, the bimetallic center accepting electrons from cytochrome *c*. Protons (both scalar and vectorial) are made available via two putative H^+-conducting pathways, identified in the crystallographic structure and denoted as K and D, from residues K319 and D91 of subunit I (*4*, *5*). These two pathways seem to play a different role in the catalytic mechanism as suggested by transient kinetics on site-directed mutants of prokaryotic oxidases (see ref *2*, *3*, and *6* for reviews).

Although the ion remained undetected by X-ray crystallography (*5*, *7*−*9*), a growing body of evidence suggests that a Cl^- ion is bound to the active site of oxidized CcOX purified in the presence of this anion. In the 1980s, EXAFS studies suggested the presence of a heavy atom (S or Cl) bridging heme a_3 and Cu_B (see, for instance, ref *10*), and Blair et al. (*11*) reported an effect of Cl^- on the redox potentials of these metals. The Cl-bound form of the enzyme displays characteristic optical and EPR spectroscopic features, and a peculiar reactivity toward external ligands (*12*, *13*); moreover, bound Cl^- prevents the fast reaction of the oxidized enzyme with nitric oxide (NO; *14*). Fabian et al. (*13*) have recently determined that (i) Cl^- binds to oxidized CcOX in a 1:1 stoichiometry, (ii) binding proceeds formally with the uptake of one H^+, and (iii) when the enzyme is subjected to a reduction−oxidation cycle, Cl^- dissociates and rebinds very slowly to oxidized CcOX in agreement with previous reports (*10*, *14*). The exact location of Cl^- within the active site is still uncertain, although it has been proposed that Cl^- may be a ligand of Cu_B (*12*, *15*, *16*). Interestingly, in the physiological Cl-free form of the enzyme, the same coordination position may be occupied by an OH^- group, as inferred from EXAFS and ENDOR studies (*15*) and suggested by a continuous electron density between heme a_3 and Cu_B seen in the crystallographic structure of oxidized *Paracoccus denitrificans* CcOX (*7*). Although the validity of an OH^- group as one of the Cu_B ligands is challenged by Yoshikawa et al. (*8*), electrostatic calculations suggested that it would become protonated upon reduction of this metal (*17*).

The redox-linked proton pumping mechanism of CcOX, still unknown in detail, clearly demands a tight coupling between electron and proton transfer within the enzyme. It is therefore not surprising that, on enzyme reduction, protons are bound by the enzyme, as predicted by the observed pH dependence of the redox potential of the metal centers (*11*). Consistently, it was reported that the complete reduction of

[†] Work partially supported by Ministero dell'Istruzione, dell'Università e della Ricerca of Italy (Programma di Ricerca Scientifica Interuniversitario Nazionale "Bioenergetica: aspetti genetici, biochimici e fisiopatologici" to P.S. and Centro di Eccellenza "Biologia e Medicina Molecolare" to M.B.).

* To whom correspondence should be addressed: Dipartimento di Scienze Biochimiche "A. Rossi-Fanelli", Università di Roma "La Sapienza", Piazzale Aldo Moro 5, I-00185 Roma, Italy. Telephone: 39-06-4450291. Fax: 39-06-4440062. E-mail: paolo.sarti@uniroma1.it.

[‡] These authors contributed equally to this work.

[1] Abbreviations: CcOX, cytochrome *c* oxidase; TAME, *N*α-*p*-tosyl-L-arginine methyl ester; EPR, electron paramagnetic resonance; EXAFS, extended X-ray absorption fine structure; ENDOR, electron−nuclear double resonance.

10.1021/bi025917k CCC: $22.00
Published on Web 10/05/2002

CcOX in detergent solution at pH 7.2−7.5 is associated with the uptake of 2.4 ± 0.1 H^+/aa_3 (*18*, *19*); of these, ∼2 H^+/aa_3 was proposed to be coupled to reduction of the heme a_3−Cu_B site and the remaining ∼0.4 H^+/aa_3 to heme *a* reduction (*18*). The H^+:heme *a* ratio is however controversial, being dependent on the redox and ligation state of the active site (*19*−*22*).

In this study, we investigate by stopped-flow spectrophotometry the effect of bound Cl^- on the kinetics and stoichiometry of the redox-linked protonation of CcOX. The results allow us to conclude that, after transfer of the first electron to the active site, one H^+ is taken up [presumably through the K pathway (*23*−*26*)] and promotes the protonation and the subsequent dissociation of Cl^- as HCl. We suggest that in the physiologically competent Cl-free state of the enzyme, an OH^- group bound to Cu_B follows the same mechanism with dissociation of H_2O, as recently proposed (*2*, *3*, *24*).

MATERIALS AND METHODS

Materials. Dodecyl β-D-maltoside was purchased from Biomol (Hamburg, Germany); Ru-II hexamine, phenol red, glucose oxidase, catalase, carbonic anhydrase, trypsin, and Nα-*p*-tosyl-L-arginine methyl ester (TAME) were from Sigma (St. Louis, MO). Experiments were performed at 20 °C and pH 7.3−7.5 in the presence of an unbuffered medium containing 20 mM K_2SO_4 and 0.2% dodecyl β-D-maltoside. Phenol red (pK_a = 7.8) was used at a concentration of 100 μM. The medium was degassed by N_2 equilibration in the presence of 10 μg/mL carbonic anhydrase (see below). Contaminant oxygen was further scavenged by addition of glucose (2 mM), glucose oxidase (4 units/mL), and catalase (260 units/mL).

Cytochrome *c* oxidase (CcOX) was purified from beef heart according to the protocol of Soulimane and Buse (*27*) and kept at −80 °C until it was used. This procedure yields mainly a Cl-bound enzyme as prepared (*13*, *14*). The Cl-free enzyme was obtained by extensive dialysis (∼2 days at 4 °C) against the above-mentioned medium, whereas chloride removal was prevented by performing the dialysis against 60 mM KCl and 0.2% dodecyl β-D-maltoside. The absence of Cl^- at the binuclear center was demonstrated by anaerobically reacting the oxidized enzyme with NO (*14*). After dialysis, the enzyme (either Cl-free or Cl-bound) was degassed by N_2 equilibration in the presence of 10 μg/mL carbonic anhydrase (see below), and immediately before the experiment, glucose, glucose oxidase, and catalase were added. The CcOX concentration was determined using an extinction coefficient difference $\Delta\epsilon_{444(red-ox)}$ of 156 mM^{-1} cm^{-1} and is expressed all throughout in terms of functional units (aa_3).

Absorption Spectroscopy. Static spectra were recorded with a double-beam spectrophotometer (Jasco V550). Stopped-flow experiments were carried out at 20 °C with a thermostated instrument (DX.17MV, Applied Photophysics, Leatherhead, U.K.), equipped with a diode array. The instrument has a 1 cm light path and can work in a sequential mixing mode, allowing two sequential mixing events with a preset time delay between them. Absorption spectra were collected with an acquisition time of 5 ms according to a logarithmic function of time up to 10 s after mixing. Data analysis was carried out using the software MATLAB (MathWorks, Natick, MA). Time-resolved spectra were fitted to a linear combination of reference spectra by using the pseudoinverse algorithm.

Calibration of the Proton Measurements. Calibration of the phenol red absorption changes was performed, in the unbuffered medium used for the experiments, according to Sarti et al. (*28*), by monitoring the trypsin-catalyzed hydrolysis of TAME, which releases one H^+ per molecule (*29*). In a typical calibration experiment, TAME at increasing concentrations (from 10 to 40 μM) was premixed with trypsin (0.6 mg/mL); after 10 ms, the resulting solution was mixed with a solution containing oxidized CcOX (10 μM aa_3) to account for the contribution of the enzyme to the overall buffer power. After the second mixing, absorption spectra were collected as a function of time. Hydrolysis of TAME causes an acidification of the medium, the extent of which is directly proportional to the TAME concentration. Data were corrected for an aspecific signal of the dye, which was always observed when diluting 1:1 oxidized CcOX in the stopped-flow apparatus. Such an aspecific signal, not related to redox reactions, corresponds to an acidification, which becomes small and highly reproducible, in both amplitudes and rates, when the content in carbonated species of the medium is lowered as much as possible. To achieve this, we boiled milli-Q water to prepare the medium and we degassed the solutions in the presence of carbonic anhydrase.

Assessment of Proton Uptake by Cytochrome Oxidase. In a typical experiment, the reduction of 10 μM degassed oxidized CcOX (aa_3) was monitored at pH 7.3−7.5 after mixing it with a solution containing Ru-II hexamine (60 μM) in the presence of 100 μM phenol red (concentration after mixing); the progress of the reaction was followed by collecting a set of 100 spectra, and data were corrected for the above-mentioned aspecific acidification. The resulting set of time-resolved spectra was clearly contributed by three chromophores: phenol red, heme *a*, and heme a_3. Deconvolution of the three optical contributions was achieved by the pseudoinverse algorithm. Every acquired difference spectrum (the baseline being the end point spectrum) was fitted to a linear combination of the following three reference spectra: the alkaline-*minus*-acid spectrum of phenol red and the reduced-*minus*-oxidized spectra of heme *a* and heme a_3 (the latter spectra being normalized to enzyme concentration). This analysis yields the time courses of each of the three chromophores, which were independently processed by curve fitting. Since in the measurements described above the enzyme is exposed to phenol red for the duration of the experiment, we verified that the dye does not interfere with the enzyme activity, even after prolonged incubation (hours).

RESULTS

The experiment was designed to measure by stopped-flow spectrophotometry the stoichiometry of H^+ uptake associated with the reduction of CcOX, either in the Cl-bound or in the Cl-free state. Proton uptake has been assessed by using the pH dye phenol red, the signal of which has been calibrated by monitoring in the visible region the trypsin-mediated hydrolysis of increasing concentrations of TAME (*28*), releasing one H^+ per molecule (*29*; see Materials and Methods for details). Linear regression of these data (not

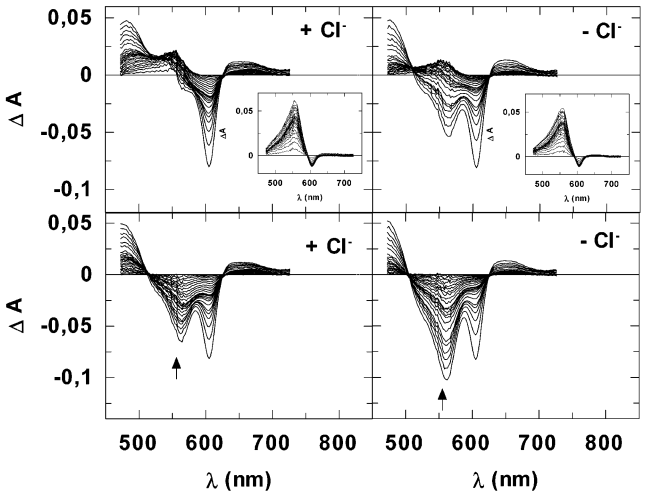

FIGURE 1: Effect of chloride on the H^+ uptake upon reduction of CcOX. The top panels display the absorption spectra collected within 10 s of mixing under anaerobic conditions of Ru-II hexamine with oxidized CcOX in the presence of phenol red with or without Cl^-. The medium consisted of 20 mM K_2SO_4 and 0.2% dodecyl β-D-maltoside. Concentrations after mixing were as follows: 5.5 μM aa_3 for CcOX, 30 μM Ru-II hexamine, and 100 μM phenol red. The spectra are shown as difference spectra with reference to the end point spectrum (acquired at 10 s). The two insets display the aspecific acidification observed over the same time range by performing the same experiment but in the absence of Ru-II hexamine (the baseline being the end point spectrum). This information was used to correct the difference spectra in the top panels. The corrected spectra, depicted in the bottom panels, show that the reduction of the Cl-bound enzyme (left) is coupled to an apparent H^+ uptake that is smaller than that observed with the Cl-free enzyme (right), as indicated by the smaller absorbance increase at ~560 nm (see the arrow).

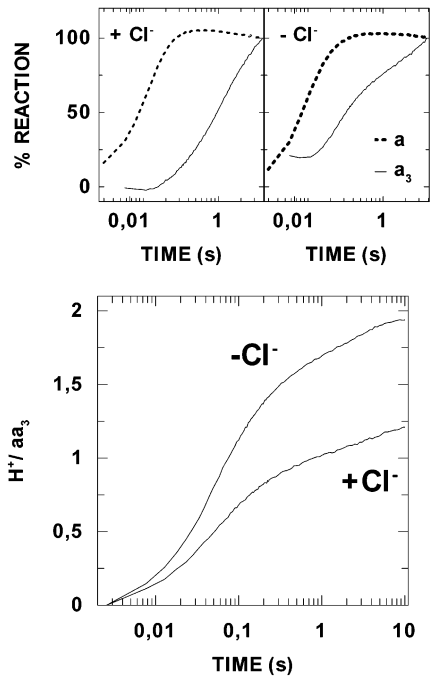

FIGURE 2: Kinetic analysis of H^+ uptake coupled to reduction of CcOX. The time-resolved spectra in Figure 1 (bottom panels) were analyzed by the pseudoinverse algorithm to separate the time courses of heme *a* and heme a_3 (top) from the time course of phenol red (bottom). In the top panels, Cl^- bound at the active site has some effect on the kinetics of heme a_3 reduction (—), but no effect on the kinetics of heme *a* reduction (- - -). In the bottom panels is shown the time course of H^+ uptake coupled to the reduction of oxidized CcOX in the presence or absence of Cl^-, obtained from the phenol red absorbance changes normalized to the enzyme concentration. Bound Cl^- lowers the extent of the apparent overall H^+ uptake.

shown) allowed determination of the difference spectrum of the dye corresponding to 1 μM H^+ released into the medium; under the chosen experimental conditions, the calibration yields a ΔA_{558} of 9.8 ± 1.6 mOD/μM H^+ (n = 16).

The H^+ uptake associated with CcOX reduction was assessed by mixing the oxidized enzyme (either Cl^--bound or Cl^--free) with Ru-II hexamine in the presence of phenol red. As shown in Figure 1, the time-resolved absorption changes in the visible region show the reduction of CcOX (~605 nm) and the deprotonation of the pH dye (~560 nm). The raw data collected in the presence of Ru-II hexamine (top panels) were corrected for the aspecific acidification signal of the dye collected in the absence of the reductant (see the insets of the top panels in Figure 1 and Materials and Methods for details); the corrected spectra are reported in the bottom panels of Figure 1. By comparison of the absorbance changes at ~560 nm, it is evident that the apparent stoichiometry of H^+ uptake in the Cl-bound enzyme is lower than that detected in the Cl-free one.

The contribution of the three chromophores (heme *a*, heme a_3, and phenol red) to the difference spectra in Figure 1 was calculated by the pseudoinverse algorithm, involving a linear combination of the reduced-*minus*-oxidized spectra of heme *a* and heme a_3 and the alkaline-*minus*-acid spectrum of phenol red. The result of this analysis is reported in Figure 2, showing the time courses of the three optical components. Data indicate that Cl^- does not affect the rate of heme *a* reduction (k ~ 35 s^{-1}; top panels in Figure 2), but has a slight effect on the kinetics of heme a_3 reduction. Regardless of the presence of Cl^-, the reduction of the latter redox center is biphasic, the two rate constants k_1 and k_2 being 7.3 and 0.33 s^{-1}, respectively, in the Cl-free enzyme and 3.2 and 0.39 s^{-1} in the Cl-bound enzyme, respectively; the fast phase accounts for 60% of the total amplitude in the Cl-free enzyme, and 35% in the Cl-bound one. The major effect of Cl^- is on the extent of H^+ uptake, which is smaller in the Cl-bound enzyme (see the bottom panel of Figure 2 and Table 1). By repeating these measurements, at different ionic strengths and reductant concentrations, we estimated the following overall apparent H^+ uptake stoichiometries: 1.40 ± 0.21 H^+/aa_3 for the Cl-bound CcOX (16 independent measurements) and 2.28 ± 0.36 H^+/aa_3 for the Cl-free enzyme (15 independent measurements).

Kinetic analysis of the time courses of CcOX reduction and phenol red deprotonation is shown in Table 1, which summarizes the results of a subset of experiments carried out under the conditions described in the legend of Figure 1. The overall time course of the pH dye deprotonation is best fitted to the sum of three exponentials, the first phase being almost synchronous with heme *a* reduction and the following two phases reasonably matching the biphasic reduction of heme a_3. Comparison of these data sets confirms that the presence of Cl^- decreases the apparent H^+ uptake stoichiometry coupled to enzyme reduction by ~0.8−0.9 H^+/aa_3. Interestingly, most of the ~0.8−0.9 extra proton observed on reduction of the Cl-free enzyme is taken up synchronously with the reduction of heme *a*, and prior to

Table 1: Kinetic Analysis of Proton Uptake Coupled to CcOX Reduction[a]

	first phase		second phase		third phase		
	k (s^{-1})	H^+/aa_3	k (s^{-1})	H^+/aa_3	k (s^{-1})	H^+/aa_3	total H^+/aa_3
Cl^--free	25 ± 4 (39 ± 8)[b]	1.19 ± 0.25	5.2 ± 1.1 (8.7 ± 2.0)[c]	0.61 ± 0.03	0.39 ± 0.07 (0.43 ± 0.11)[c]	0.42 ± 0.16	2.22 ± 0.32 ($n = 5$)[d]
Cl^--bound	32 ± 6 (34 ± 2)[b]	0.57 ± 0.02	7.1 ± 2.7 (3.6 ± 0.7)[c]	0.54 ± 0.18	0.44 ± 0.22 (0.42 ± 0.03)[c]	0.27 ± 0.04	1.38 ± 0.15 ($n = 3$)[d]

[a] Experimental conditions as described in the legend of Figure 1. The time course of phenol red was fitted to the sum of three exponentials, and the resulting rate constants and amplitudes are reported with their standard deviations. The first phase is almost synchronous to heme *a* reduction, whereas the other two phases match the heme a_3 reduction. These data in dodecyl β-D-maltoside indicate that bound chloride reduces the overall apparent stoichiometry of H^+ uptake with a major effect at the first phase. [b] Rate constant of heme *a* reduction. [c] Rate constant of heme a_3 reduction. [d] Number of experiments.

the reduction of heme a_3 (compare the H^+/aa_3 values relative to those of the first phase in Table 1). Nevertheless, under the chosen experimental conditions (i.e., with dodecyl β-D-maltoside, at pH 7.3−7.5, and with a low reductant concentration), it is difficult to assign unequivocally these extra protons to the reduction of either heme *a* or the heme a_3−Cu_B site. This is due to the fact that using CcOX solubilized in dodecyl β-D-maltoside, the rate constant for the reduction of the heme a_3−Cu_B site [ranging from ~25 to ~85 s^{-1} at pH 7 (*30*, *31*)] is comparable to the observed rate constant at which heme *a* is reduced ($k' \sim 35$ s^{-1} at 30 μM Ru-II hexamine). Under these conditions, a significant fraction of Cu_B is expected to be reduced synchronously with heme *a*, thus increasing the apparent H^+ uptake stoichiometry at the first phase (Table 1).

To separate the relative contributions of heme *a* and the heme a_3−Cu_B site to the overall redox-linked H^+ uptake, dodecyl β-D-maltoside was replaced with Triton X-100, a detergent causing a remarkable slowdown of the electron transfer between heme *a* and the active site (*32*), correlating with a reduced enzyme activity. Under these experimental conditions, reduction of heme *a* is definitely time-resolved from the reduction of the heme a_3−Cu_B site, and the H^+/heme *a* stoichiometry can be better estimated. In Figure 3, the time courses of phenol red at increasing concentrations of Ru-II hexamine are displayed. In agreement with the experiments in dodecyl β-D-maltoside, the overall apparent H^+ uptake for the Cl-bound enzyme is smaller than that detected for the Cl-free CcOX. Over the first 40 ms of the reaction, heme *a* is reduced at a rate proportional to the concentration of the reductant (solid line, insets of Figure 3); at each reductant concentration, almost synchronously with heme *a* reduction, the same amount of protons (0.59 ± 0.06 H^+/aa_3, $n = 11$) is taken up regardless of the presence or absence of Cl^- at the active site. On this basis, we assign the uptake of this 0.59 ± 0.06 proton to the reduction of heme *a*.

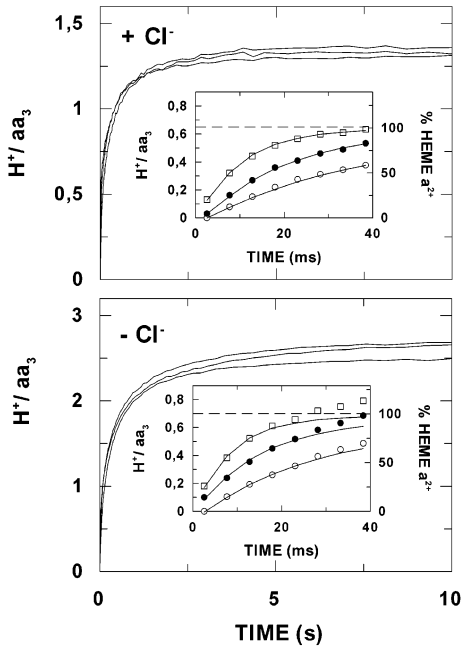

FIGURE 3: H^+ uptake coupled to heme *a* reduction is not affected by bound chloride. Degassed oxidized CcOX (4.7 μM after mixing) was anaerobically mixed in the stopped-flow apparatus, in the presence of 100 μM phenol red, with increasing concentrations of Ru-II hexamine. Dodecyl β-D-maltoside was replaced with 0.1% Triton X-100 to slow the rate of reduction of heme a_3. The data confirm that, independent of the reductant concentration, the overall redox-linked H^+ uptake is smaller for the Cl-bound enzyme (top) than for the Cl-free enzyme (bottom). In the insets, the time course of the reduction of heme *a* over the first 40 ms (−) is proportional to the reductant concentration; synchronously with heme *a* reduction, ~0.6−0.7 H^+/aa_3 is taken up (symbols), both in the Cl-bound (top) and in the Cl-free enzyme (bottom). Reduction of heme a_3 under these conditions is much slower. The concentration of Ru-II hexamine after mixing was 30 (○), 60 (●), or 125 μM (□). Data show that Cl^- bound at the active site of CcOX does not significantly affect the extent of H^+ uptake coupled to the reduction of heme *a*.

DISCUSSION

In this paper, we report new data on the effect of bound Cl^- on the stoichiometry and the kinetics of redox-linked protonation of soluble CcOX, studied by multiwavelength stopped-flow spectroscopy and using the pH dye phenol red. The experiment to determine the stoichiometry of H^+ uptake upon reduction of CcOX, either Cl-bound or Cl-free, makes use of Ru-II hexamine as a non-H^+-releasing electron donor. We found that the overall reduction of the Cl-bound enzyme is coupled to an apparent H^+ uptake of 1.40 ± 0.21 H^+/aa_3, which is ~0.9 H^+ smaller than that of the Cl-free enzyme (uptake of 2.28 ± 0.36 H^+/aa_3), in agreement with the literature (*18*, *19*). As explained below, we propose that the smaller H^+ uptake observed in the Cl-bound enzyme is caused by the release into the bulk of ~1 H^+, accompanying the dissociation of HCl from the protein upon reduction of Cu_B.

Since both heme *a* and the heme a_3−Cu_B site contribute to the overall redox-linked H^+ uptake, we separated kinetically these two contributions by monitoring the reaction under experimental conditions in which heme *a* reduction was time-resolved from the reduction of the active site. For

this purpose, we have employed CcOX solubilized in Triton X-100, a detergent causing a slow redox equilibration between heme *a* and the active site. As demonstrated by Malatesta et al. (*32*), Triton X-100 acts by delaying the reduction of both Cu_B and heme a_3, resulting in a slower enzyme turnover, although the molecular basis for such an effect is still unknown. Taking advantage of this peculiar effect of Triton X-100, in the investigation presented here we were able to show that, regardless of the presence or absence of bound Cl^-, 0.59 ± 0.06 proton is taken up synchronously with the reduction of heme *a* at a rate proportional to the reductant concentration (Figure 3). We thus conclude that the reduction of this site is coupled to the uptake of ~0.6 H^+. The H^+:heme *a* ratio is rather controversial in the literature, particularly when measured in the mixed-valence CO adduct of the enzyme, with the active site in the reduced state (*19*, *21*, *22*). The value estimated by us is slightly higher than, but not inconsistent with, the value of ~0.4 H^+/aa_3 measured by Mitchell and Rich (*18*). There is no consensus about the pathway through which this proton is taken up. Blocking either the K or D pathway by site-directed mutagenesis has no effect on the rate of heme *a* reduction (*24*, *26*), suggesting that these protons are transferred through an alternative pathway; however, Ruitenberg et al. (*23*) proposed the involvement of the K pathway. The Helsinki group suggested that these protons are taken up from the P phase (*21*), but the Bari group claims that the uptake is from the N phase (see ref *20* for a review).

The overall picture emerging from our data is therefore as follows. We observe (i) ~0.6 H^+/aa_3 taken upon reduction of heme *a*, (ii) ~0.8 H^+/aa_3 taken upon reduction of the active site if Cl^- is bound, and (iii) an increase in the latter value to ~1.7 H^+/aa_3 if Cl^- is removed. Thus, Cl^- bound to CcOX decreases the overall H^+ uptake stoichiometry by lowering the extent of the apparent H^+ uptake coupled to the reduction of the binuclear site, without changing the number of protons taken up on reduction of heme *a*. Now it may be wondered whether the effect of Cl^- is on the reduction of either heme a_3 or Cu_B. When the data for the enzyme solubilized in dodecyl β-D-maltoside are considered, where electron transfer from heme *a* to the active site is much faster than in the presence of Triton X-100 (*30*−*32*), the effect of bound Cl^- on the overall H^+ uptake is still observed, as well as the ~0.6 H^+/aa_3 taken up as a result of heme *a* reduction with the Cl-bound enzyme (Figure 2 and Table 1). If Cl^- is removed, an extra ~0.9 H^+/aa_3 disappears from the bulk upon CcOX reduction, mostly detected *prior* to heme a_3 reduction and almost synchronously with the reduction of heme *a* (see Table 1). This is expected, since under these conditions (i.e., with dodecyl β-D-maltoside and at low reductant concentrations), electron equilibration between heme *a* and the active site proceeds at a rate [ranging at pH 7 from ~25 to ~85 s^{-1} (*30*, *31*)] comparable to the rate at which heme *a* is reduced ($k' \sim 35\ s^{-1}$ at 30 μM Ru-II hexamine). Therefore, a significant fraction of the heme a_3−Cu_B site is reduced synchronously with heme *a* accounting for the extra H^+ uptake. Thus, with the enzyme solubilized in dodecyl β-D-maltoside, most of the extra ~0.9 H^+/aa_3 proton seen on Cl^- removal is taken up *prior* to heme a_3 reduction, but cannot be assigned to the reduction of heme *a*. On this basis, we conclude that bound Cl^- affects the H^+ uptake coupled to the reduction of Cu_B, the metal being preferentially reduced in the single-electron reduced active site.

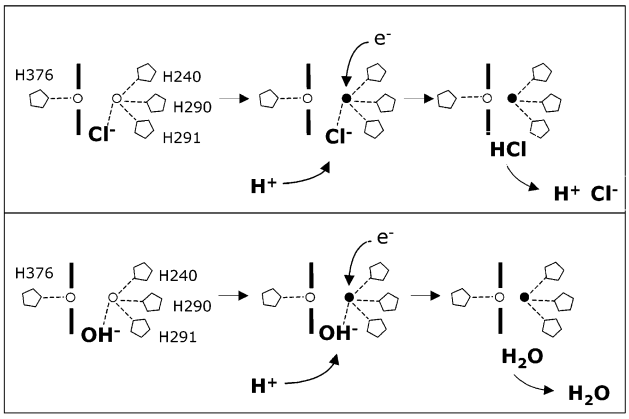

FIGURE 4: Possible model in which the active site of CcOX, either in the Cl-bound (top) or in the Cl-free form (bottom), is schematically drawn with heme a_3 and Cu_B, depicted with their crystallographically determined histidine ligands. The redox state of the two metals is denoted by empty (oxidized) or filled circles (reduced). In the fully oxidized site, Cu_B has a fourth ligand, which is either Cl^- (top) or OH^- (bottom). When the first electron is transferred to the active site, Cu_B is reduced and, concomitantly, the anionic Cu_B ligand (OH^- or Cl^-) dissociates, picks up one proton, and diffuses as an electroneutral molecule (H_2O or HCl) from the protein into the bulk. Once released into the bulk, HCl dissociates releasing one proton back into the medium.

This hypothesis is depicted in Figure 4, where oxidized Cu_B (liganded to H240, H290, and H291 of subunit I) coordinates either OH^- in the Cl-free CcOX (*15*) or Cl^- in the Cl-bound enzyme (*12*, *15*, *16*). If the first electron transferred to the active site resides preferentially on Cu_B, the reduction of this metal is coupled to the dissociation of either OH^- or Cl^-, charge-neutralized by protonation and thus dissociating as either H_2O or HCl. Once released, HCl will completely dissociate one proton to the aqueous phase, which explains why the net proton uptake in the Cl-bound enzyme is lower than in the Cl-free enzyme.

We point out that H_2O formation on Cu_B reduction, though tentatively proposed in the past (*2*, *3*, *24*), has never been demonstrated; the data for the Cl-bound enzyme herein reported, being fully compatible with it, represent experimental support for such a mechanism. It is also worth noticing that, at variance from a previous proposal (see Figure 3 of ref *2*), this study seems to indicate that arrival of the first electron to the active site is sufficient to promote the dissociation of H_2O or HCl into the bulk. In other words, H_2O dissociation in the reductive part of the catalytic cycle already occurs upon formation of the single-electron reduced active site (**E**), i.e., prior to transfer of the second electron. The model in Figure 4 not only provides an explanation for the results obtained in the investigation presented here but also is consistent with other experimental evidence in the literature. That Cl^- might be a ligand of Cu_B, although never assessed crystallographically, has been inferred from its effects on the reactivity toward external ligands targeting this metal (see, for instance, refs *12*−*14*) and confirmed by EPR, EXAFS, and ENDOR (*10*, *15*, *16*). The proposed model (Figure 4) accounts for the finding that Cl^- dissociation proceeds with the release of 1 H^+, as suggested by Fabian et al. (*13*) to explain the pH dependence of the

dissociation constant for the formation of the Cl-bound enzyme. However, at variance with Fabian et al. (*13*), the pH dependence of Cl^- *binding* to the oxidized enzyme may be coupled to the net dissociation of 1 OH^-, rather than to the net uptake of 1 H^+. Competing for the same metal, Cl^- binding to oxidized CcOX should displace the OH^- bound to Cu_B, causing its dissociation into the bulk. Finally, the model proposed in Figure 4 includes the finding that a reduction−reoxidation cycle of CcOX is associated with Cl^- dissociation (*10*, *13*, *14*), due to the decreased affinity of Cl for the single-electron reduced active site, suggested by Blair et al. (*11*).

That OH^- might be a ligand of Cu_B in the fully oxidized active site of CcOX was inferred from EXAFS and ENDOR experiments (*15*) and is consistent with the proposal of Ostermeier et al. (*7*), who modeled a water plus a OH^- bridging heme a_3 and Cu_B. This interpretation is however opposed by Yoshikawa et al. (*8*), who proposed a bridging peroxide. Further experimental evidence for an OH^- group at the active site of CcOX has recently been acquired by performing laser-triggered reverse electron transfer experiments on site-directed mutants of the K pathway of the *Rhodobacter sphaeroides* enzyme (*38*). Additionally, electrostatic calculations reported by Kannt et al. (*17*) strongly favor OH^- as a Cu_B ligand, with stabilization of the fully oxidized active site achieved by decreasing the level of electrostatic repulsion between Fe^{3+} and Cu_B^{2+} (*2*). Kannt et al. (*17*) predict dissociation and protonation of this OH^- when Cu_B is reduced by transfer of a single electron to the active site, which is relevant to the model proposed in Figure 4. Such a protonation occurs via the H^+-conducting K pathway, as assessed by site-directed mutagenesis (*23*−*26*), and promotes the subsequent dissociation of the newly formed H_2O. Alternatively, following a quantum mechanical study of O−O bond scission (*33*), Wikström and co-workers (*24*) suggested that the OH^- group bound to oxidized Cu_B is protonated by the nearby aquo ligand of heme a_3, while the proton transferred through the K pathway is delivered to the heme a_3 farnesyl hydroxyl group H-bonded to Y244. Whatever the detailed molecular mechanism, the resulting H_2O molecule dissociates and, consistently, the continuous electron density between heme a_3 and Cu_B is no longer visible in the reduced state (*8*, *34*).

It is interesting to observe that OH^- protonation that is synchronous with Cu_B reduction may have a role in the enzyme mechanism, by ensuring tight coupling between electron and proton transfer on single reduction of the active site, and accounting also for the pH-dependent rate of internal electron transfer to the oxidized active site (*31*, *32*). The model in Figure 4 implies that, following the transfer of the first electron to the active site, Cu_B changes its coordination from tetragonal to trigonal. This structural rearrangement might increase the reorganizational energy associated with this electron transfer process, possibly accounting for the slow electron transfer rates observed with the oxidized binuclear site, despite the relatively short heme *a*-to-heme a_3−Cu_B distance (*30*, *31*, *35*). Alternatively, it was proposed that the internal electron transfer from the heme a−Cu_A site to the heme a_3−Cu_B site may be rate-limited by proton diffusion through the protein matrix (*31*, *35*). The data herein reported are consistent with this hypothesis which however is not proven by the finding that internal electron transfer and H^+ uptake occur synchronously (*35*). Finally, a specific role for the H_2O molecule formed in situ cannot be ruled out. In this context, it was proposed that this H_2O molecule, once released from Cu_B, would diffuse through the protein matrix by transiently restoring the H^+ connectivity between the D pathway and the active site, which is possibly essential for proton pumping (*36*, *37*).

In conclusion, within the limits of the assumption that Cl^- may replace OH^- as a ligand of oxidized Cu_B, still inconsistent with X-ray crystallography, the data reported above strongly suggest that when the *first* electron is transferred to the active site of CcOX and Cu_B is reduced, the bound anionic ligand (OH^- or Cl^-) dissociates, picks up a H^+, diffuses as an electroneutral molecule (H_2O or HCl), from the protein into the bulk, where HCl dissociation would explain the apparent loss in the number of protons taken upon reduction of the binuclear site.

ACKNOWLEDGMENT

We thank B. Ludwig (Frankfurt, Germany) for critical reading of the manuscript.

REFERENCES

1. Ferguson-Miller, S., and Babcock, G. T. (1996) *Chem. Rev. 96*, 2889−2907.
2. Michel, H. (1999) *Biochemistry 38*, 15129−15140.
3. Zaslavsky, D., and Gennis, R. B. (2000) *Biochim. Biophys. Acta 1458*, 164−179.
4. Iwata, S., Ostermeier, C., Ludwig, B., and Michel, H. (1995) *Nature 376*, 660−669.
5. Tsukihara, T., Aoyama, H., Yamashita, E., Tomizaki, T., Yamaguchi, H., Shinzawa-Itoh, K., Nakashima, R., Yaono, R., and Yoshikawa, S. (1996) *Science 272*, 1136−1144.
6. Pfitzner, U., Odenwald, A., Ostermann, T., Weingard, L., Ludwig, B., and Richter, O. M. (1998) *J. Bioenerg. Biomembr. 30*, 89−97.
7. Ostermeier, C., Harrenga, A., Elmer, U., and Michel, H. (1997) *Proc. Natl. Acad. Sci. U.S.A. 94*, 10547−10553.
8. Yoshikawa, S., Shinzawa-Itoh, K., Nakashima, R., Yaono, R., Yamashita, E., Inoue, N., Yao, M., Fei, M. J., Peters Libeu, C., Mizushima, T., Yamaguchi, H., Tomizaki, T., and Tsukihara, T. (1998) *Science 280*, 1723−1729.
9. Soulimane, T., Buse, G., Bourenkov, G. P., Bartunik, H. D., Huber, R., and Than, M. E. (2000) *EMBO J. 19*, 1766−1776.
10. Scott, R. A., Li, P. M., and Chan, S. I. (1988) *Ann. N.Y. Acad. Sci. 550*, 53−58.
11. Blair, D. F., Ellis, W. R., Wang, H., Gray, H. B., and Chan, S. I. (1986) *J. Biol. Chem. 261*, 11524−11537.
12. Moody, A. J., Cooper, C. E., and Rich, P. R. (1991) *Biochim. Biophys. Acta 1059*, 189−207.
13. Fabian, M., Skultety, L., Brunel, C., and Palmer, G. (2001) *Biochemistry 40*, 6061−6069.
14. Giuffrè, A., Stubauer, G., Brunori, M., Sarti, P., Torres, J., and Wilson, M. T. (1998) *J. Biol. Chem. 273*, 32475−32478.
15. Fann, Y. C., Ahmed, I., Blackburn, N. J., Boswell, J. S., Verkhovskaya, M. L., Hoffman, B. M., and Wikström, M. (1995) *Biochemistry 34*, 10245−10255.
16. Butler, C. S., Seward, H. E., Greenwood, C., and Thomson, A. J. (1997) *Biochemistry 36*, 16259−16266.
17. Kannt, A., Lancaster, R. D., and Michel, H. (1998) *Biophys. J. 74*, 708−721.
18. Mitchell, R., and Rich, P. R. (1994) *Biochim. Biophys. Acta 1186*, 19−26.
19. Capitanio, N., Vygodina, T. V., Capitanio, G., Konstantinov, A. A., Nicholls, P., and Papa, S. (1997) *Biochim. Biophys. Acta 1318*, 255−265.
20. Papa, S., and Capitanio, N. (1998) *J. Bioenerg. Biomembr. 30*, 109−119.

21. Verkhovsky, M. I., Belevich, N., Morgan, J. E., and Wikström, M. (1999) *Biochim. Biophys. Acta 1412*, 184−189.
22. Capitanio, N., Capitanio, G., Boffoli, D., and Papa, S. (2000) *Biochemistry 39*, 15454−15461.
23. Ruitenberg, M., Kannt, A., Bamberg, E., Ludwig, B., Michel, H., and Fendler, K. (2000) *Proc. Natl. Acad. Sci. U.S.A. 97*, 4632−4636.
24. Wikström, M., Jasaitis, A., Backgren, C., Puustinen, A., and Verkhovsky, M. I. (2000) *Biochim. Biophys. Acta 1459*, 514−520.
25. Verkhovsky, M. I., Tuukkanen, A., Backgren, C., Puustinen, A., and Wikström, M. (2001) *Biochemistry 40*, 7077−7083.
26. Giuffrè, A., Barone, M. C., Brunori, M., D'Itri, E., Ludwig, B., Malatesta, F., Müller, H., and Sarti, P. (2002) *J. Biol. Chem. 277*, 22402−22406.
27. Soulimane, T., and Buse, G. (1995) *Eur. J. Biochem. 227*, 558−595.
28. Sarti, P., Jones, M. G., Antonini, G., Malatesta, F., Colosimo, A., Wilson, M. T., and Brunori, M. (1985) *Proc. Natl. Acad. Sci. U.S.A. 82*, 4876−4880.
29. Hummel, B. C. V. (1959) *Can. J. Biochem. Physiol. 37*, 1393−1399.
30. Brunori, M., Giuffrè, A., D'Itri, E., and Sarti, P. (1997) *J. Biol. Chem. 272*, 19870−19874.
31. Verkhovsky, M. I., Morgan, J. E., and Wikström, M. (1995) *Biochemistry 34*, 7483−7491.
32. Malatesta, F., Sarti, P., Antonini, G., Vallone, B., and Brunori, M. (1990) *Proc. Natl. Acad. Sci. U.S.A. 87*, 7410−7413.
33. Blomberg, M. R. A., Siegbahn, P. E. M., Babcock, G. T., and Wikström, M. (2000) *J. Am. Chem. Soc. 122*, 12848−12858.
34. Harrenga, A., and Michel, H. (1999) *J. Biol. Chem. 47*, 33296−33299.
35. Brzezinski, P. (1996) *Biochemistry 35*, 5611−5615.
36. Backgren, C., Hummer, G., Wikström, M., and Puustinen, A. (2000) *Biochemistry 39*, 7863−7867.
37. Gennis, R. B. (1998) *Biochim. Biophys. Acta 1365*, 241−248.
38. Sigurdson, H., Brändén, M., Namslauer, A., and Brzezinski, P. (2002) *J. Inorg. Biochem. 88*, 335−342.

BI025917K